LUND UNIVERSITY

Single Antenna Anchor-Free UWB Positioning based on Multipath Propagation

Kuang, Yubin; Åström, Karl; Tufvesson, Fredrik

Published in:
[Host publication title missing]

2013

Link to publication

Citation for published version (APA):
Kuang, Y., Åström, K., & Tufvesson, F. (2013). Single Antenna Anchor-Free UWB Positioning based on Multipath Propagation. In *[Host publication title missing]* IEEE - Institute of Electrical and Electronics Engineers Inc..

Total number of authors:
3

General rights
Unless other specific re-use rights are stated the following general rights apply:
Copyright and moral rights for the publications made accessible in the public portal are retained by the authors and/or other copyright owners and it is a condition of accessing publications that users recognise and abide by the legal requirements associated with these rights.
• Users may download and print one copy of any publication from the public portal for the purpose of private study or research.
• You may not further distribute the material or use it for any profit-making activity or commercial gain
• You may freely distribute the URL identifying the publication in the public portal

Read more about Creative commons licenses: https://creativecommons.org/licenses/

Take down policy
If you believe that this document breaches copyright please contact us providing details, and we will remove access to the work immediately and investigate your claim.

LUND UNIVERSITY

PO Box 117
221 00 Lund
+46 46-222 00 00

Download date: 12. Oct. 2024

Single Antenna Anchor-Free UWB Positioning based on Multipath Propagation

Yubin Kuang, Kalle Åström
Centre for Mathematical Sciences
Lund University, Sweden
{yubin,kalle}@maths.lth.se

Fredrik Tufvesson
Dept. of Electrical and Information Technology
Lund University, Sweden
Fredrik.Tufvesson@eit.lth.se

***Abstract*—Radio based localization and tracking usually require multiple receivers/transmitters or a known floor plan. This paper presents a method for anchor free indoor positioning based on single antenna ultra wideband (UWB) measurements. By using time of arrival information from multipath propagation components stemming from scatterers with different, but unknown, positions we estimate the movement of the receiver as well as the angle of arrival of the considered multipath components. Experiments are shown for real indoor data measured in a lecture room with promising results. Simultaneous estimation of both receiver motion, transmitter and scatterer positions is performed using an factorization based approach followed by non-linear least squares optimization. A RANSAC approach to automatic matching of data has also been implemented and tested. The resulting reconstruction is compared to ground truth motion as given by the antenna positioner. The resulting accuracy is in the order of one cm.**

***Index Terms*—ultra wideband, tracking, localization, multipath, time of arrival, TOA, structure from motion**

I. Introduction

Radio based localization, tracking and sensor network calibration using ultra wideband (UWB) and time of arrival (TOA) or time difference of arrival (TDOA) measurements has been studied extensively. Usually, the position estimates are based on delay estimates of the first arriving component from several sources, and some kind of trilateration is performed to get the position estimates. An overview of different positioning and localization methods can be found in [1]. Due to the existence of multipath transmission, the fundamental limits of ranging and localization using wideband signals are studied extensively in [2], [3]. There are, however, also approaches where delays of multipath components are used [4] to estimate the position of a transmitter or a receiver. In [5] a positioning method is presented based on a single source delay measurements and floorplan information. By using the concept of virtual sources, whose locations were known through the floorplan, a single antenna receiver was positioned and tracked. The method proposed in this paper extends those ideas, but without using floorplan information. The directions to the virtual sources, the scatterers, are instead estimated based on so called structure from motion techniques from node localization in sensor networks. For those networks, there is usually an initialization process where positions of the nodes are estimated. The initialization problem based on TOA measurements in sensor networks has been studied in [6], where solutions to the minimal case of three transmitters and three receivers in the plane is given, but no practical solver for the minimal case in 3 dimensions (3D) is provided. Initialization based on TDOA and TOA measurements is studied in [7], where solutions were given to non-minimal cases, e.g. ten receivers and five transmitters in 3D. A line of previous works impose additional assumptions on the measurements. By assuming that a pair of receiver and transmitter has the same location, a closed form solution is proposed in [8] for TOA based positioning in 3D. In [9] and refined in [10], far field approximation (assuming that the distances from the transmitters to receivers are considerably larger than the distances between receivers) was utilized to solve both the TOA and TDOA problems. Also in [11] the node localization problem is solved when neither transmitters and receivers are synchronized in the far-field setting. to get approximate locations of sensor positions as initialization.

In this paper we present a method for anchor free positioning using UWB measurements from one single transmitter to a single moving receiver. The receiver estimates the delays of the major multipath components (MPCs) by a detect and subtract based method [12] and the delay changes of those MPCs are then tracked. Simultaneous estimation of both receiver motion and transmitter positions and its reflections are performed using a factorization based approach followed by non-linear least squares optimization. A RANSAC [13] approach to automatic matching of data has also been implemented and tested. Experiments are shown for real data with promising results. The method has been tested on indoor UWB measurements from a furnished lecture room. The motion of the receiver is controlled by a 3D positioner which gives ground truth motion with an accuracy of 50 μm. As a proof of concept, and due to practical constraints with the positioner, the movements are limited to a cube measuring 0.30 x 0.30 x 0.30 m^3. The resulting reconstruction of the movement is compared to ground truth motion as given by the positioner. The resulting accuracy is in the order of one cm.

The remainder of the paper is organized as follows. In Sec. II we describe the model for the measured impulse responses, and the method of extracting the delays of the multipath components. In Sec. III the process of relating the measured delays is described and in Sec. IV the theory for structure from motion algorithms is discussed. Measurements and estimation

results are discussed in Sec. V and, finally, the conclusions in Sec. VI wrap up the paper.

II. Signal model

If we assume that pulse distortion can be neglected, the impulse response of the UWB channel can be modeled as [14]

$$h(\tau, t) = \sum_l \alpha_l(t)\delta(\tau - \tau_l(t)), \tag{1}$$

where t denotes time, $\delta(\cdot)$ is the Kronecker delta function, $\alpha_l(t)$ and $\tau_l(t)$ are the channel gain and delay of the lth multipath component (MPC), respectively. We assume that the scatterers in the environment and the transmitter (Tx) are fixed during the movement of the receiver (Rx), and hence that the only change of the impulse is due to movements of the Rx (or vice versa). The impulse response is sampled at different positions in space, and we replace the time continuous variable t with a sample index i. For the tracking method described later on, we further assume that there is a maximum movement between the samples of the impulse response. For the position tracking, for each i we extract the gains, $\alpha_{i,k}$, and delays, $\tau_{i,k}$, of the 100 strongest MPCs from the impulse responses by the method described in [12]. This method is basically is a variant of the CLEAN algorithm [15], and is based on a detect and subtract approach when extracting the MPCs. The major MPCs typically stem from the dominating scatterers in the environment and the change of delay between successive samples of a particular MPC reflects the movement of the antenna in relation to this scatterer.

III. Finding correspondences among mulitpath components

After multiplication with the speed of light c, each delay corresponds to a propagation distance $d_{i,k} = c\tau_{i,k}$, between the transmitter and receiver for that particular MPC, possibly as it has been scattered and reflected in the surroundings. Each scatterer, being a planar surface or a smaller reflecting object, gives rise to a virtual transmitter position $\mathbf{s}_j$. If one can find the correspondences, i.e. for each virtual transmitter $\mathbf{s}_j$ can find all those distances $d_{i,j}$, then one obtains a structure from motion problem of the following type: Given measurements $d_{i,j}$ determine both transmitter positions $\mathbf{s}_j$ and receiver positions $\mathbf{r}_i$ such that

$$d_{i,j} = |\mathbf{r}_i - \mathbf{s}_j|.$$

Such inverse problems have received increased attention in the last decade. A brief overview of the state-of-the-art and some of the most relevant methods are presented in the next section.

IV. Structure from motion algorithms

Again assume that $\mathbf{r}_i$, $i = 1, \ldots, m$ and $\mathbf{s}_j$, $j = 1, \ldots, n$ be the spatial coordinates of m receivers and n transmitters, respectively. For the measured distances $d_{i,j}$ from receiver $\mathbf{r}_i$ and transmitter $\mathbf{s}_j$, we have $d_{i,j} = |\mathbf{r}_i - \mathbf{s}_j|$.

For the general problem there are some results concerning minimal data needed in the planar case, [6]. It is shown that 3 receivers and 3 transmitters can be placed in four configurations to fit the data. In 3D there are both results that can be used as long as there is data from at least 4 (or 10) transmitters to 10 (or 4) receivers, cf. [7].

If during the measurements, the relative motion of say the receiver, is small in comparison with the distance d between the receiver $\mathbf{r}$ and the transmitter $\mathbf{s}$, it is reasonable to approximate the distance $d = |\mathbf{r}-\mathbf{s}| \approx |\mathbf{r}_0-\mathbf{s}|+(\mathbf{r}-\mathbf{r}_0)^T\mathbf{n} = \mathbf{r}^T\mathbf{n} + (|\mathbf{r}_0 - \mathbf{s}| - \mathbf{r}_0^T\mathbf{n})$. Here $\mathbf{r}_0$ is the 3D position of a reference receiver position and $\mathbf{n}$ is the direction from the receivers towards the transmitter, now assumed to be independent of receiver position and with unit length. By setting $o = |\mathbf{r}_0 - \mathbf{s}| - \mathbf{r}_0^T\mathbf{n}$, one obtains the far field approximation

$$d(\mathbf{n}, \mathbf{r}) \approx \mathbf{r}^T\mathbf{n} + o.$$

Here, we see can that o is an unknown constant related to each transmitter via $\mathbf{n}$.

The far-field structure from motion problem is thus: Given distance measurements d_{ij} estimate the motion of the receiver r_i and the direction n_j and offsets o_j to the transmitters such that

$$d_{i,j} \approx \mathbf{r}_i^T\mathbf{n}_j + o_j.$$

The far-field structure from motion problem has been treated in [9] and the critical configurations of such reconstructions has been studied in [10].

Lemma 4.1: A problem with m receiver positions to n transmitters with unknown constant o_j can without loss of generality be converted to a problem with $m-1$ measurements to n base stations with known constant.

Proof: Note that because of the unknown constant o_j the problem does not change in character by modification $\bar{d}_{i,j} = d_{i,j} - K_j$. For simplicity we set $\bar{d}_{i,j} = d_{i+1,j} - d_{1,j} = (\mathbf{r}_{i+1,j} - \mathbf{r}_1)^T\mathbf{n}_j = \mathbf{r}_{i+1,j}^T\mathbf{n}_j + \bar{o}_j$, where $i = 1, \ldots, m-1$ and $\bar{o}_j = -\mathbf{r}_1^T\mathbf{n}_j$. By also setting $\mathbf{r}_1 = \begin{pmatrix} 0 & 0 & 0 \end{pmatrix}^T$, we get $\bar{o}_j = 0$ or equivalently $\bar{d}_{i,j} = \mathbf{r}_{i+1}^T\mathbf{n}_j$. This is equivalent to choosing the origin of the unknown coordinate system to the first point. ■

Thus we can without loss of generality solve the simpler problem

$$\bar{d}_{i,j} \approx \mathbf{r}_i^T\mathbf{n}_j.$$

Lemma 4.2: For measurements in 3D, the matrix $\bar{\mathbf{D}}$ with elements $\bar{d}_{i,j}$ is of rank at most 3.

Proof: The measurement equations are $\bar{d}_{i,j} = \mathbf{r}_i^T\mathbf{n}_j$. By setting

$$\mathbf{R} = \begin{pmatrix} \mathbf{r}_1 & \mathbf{r}_2 & \ldots & \mathbf{r}_m \end{pmatrix}$$

and

$$\mathbf{N} = \begin{pmatrix} \mathbf{n}_1 & \mathbf{n}_2 & \ldots & \mathbf{n}_n \end{pmatrix}$$

we see that $\bar{\mathbf{D}} = \mathbf{R}^T\mathbf{N}$. Both $\mathbf{R}$ and $\mathbf{N}$ have at most rank 3, therefore the same holds for $\bar{\mathbf{D}}$. ■

Accordingly, we have Algorithm 4.1 for the minimal case of the problem. For planar problems the same algorithm can be used. The only difference is that the matrix in Step 3 is of rank 2 and that the symmetric matrix B of size 2×2 has three degrees of freedom.

Algorithm 4.1: **Far Field TDOA Minimal Case (3D)**

Given the measurement matrix D of size 4×6.

1) Set $\bar{\mathbf{D}}_{i,j} = d_{i,j} - d_{1,j}$
2) Remove the first row of $\bar{\mathbf{D}}$
3) Calculate a singular value decomposition $\bar{\mathbf{D}} = \mathbf{USV}^T$.
4) Set $\tilde{\mathbf{R}}$ to first 3 columns of $\mathbf{U}$ and $\tilde{\mathbf{N}}$ to first 3 columns of $\mathbf{SV}^T$.
5) Solve for the six unknowns in the symmetric matrix $\mathbf{B}$ using the 6 linear constraints $\tilde{\mathbf{n}}_j^T \mathbf{B} \tilde{\mathbf{n}}_j = 1$.
6) Calculate $\mathbf{A}$ by Cholesky factorization of $\mathbf{B}$, so that $\mathbf{A}^T\mathbf{A} = \mathbf{B}$.
7) Transform motion according to $\mathbf{R} = (\tilde{\mathbf{R}}\mathbf{A}^{-1})^T$ and structure according to $\mathbf{N} = \mathbf{A}\tilde{\mathbf{N}}$.

V. Experiments

A. Measurement Setup

Measurements were conducted in a furnished lecture room of size 8.1 x 6.3 x 2.6 m^3 (Fig. 1). A transmit antenna at a height of 1.47 m was put in the middle of the lecture room. The receiver antenna is put at a distant on a straight line of sight away from it, the x direction. The receiving antenna first moves linearly in x, y, z directions and then moves on the surface of xy, xz and yz, making a shape of square on each surface. The steps between successive antenna positions are 1 cm each, but not that we make no assumptions on the movements other than that there is a maximum distance between measurements. The measurements were performed with an HP 8720C vector analyzer (VNA) using SkyCross UWB antennas SMT-3TO10M-A at both the Tx and Rx end. The VNA measures S_{21}, the channel transfer function, for 1601 frequency points, sweeping the whole bandwidth of 3.1 GHz to 10.6 GHz. Note that the expected delay resolution, as measured by the inverse of the bandwidth is 133 ps, corresponding to a distance of 4 cm. The IF bandwidth was set to 100 Hz in order to minimize the impact of noise. The environment was static during the measurements and except for the moving receiver there are no other movements in the close environment. The measurements of the matching strength between transmitted and received signal are shown in Fig. 2 (Left).

B. Data Processing

The result from the signal matching are the travel times $\tau_{i,k}$ for the 100 strongest peaks $i = 1, \ldots, 100$ at each of the 404 measurements positions, $k = 1, \ldots, 404$. These are shown in Fig. 2 (*right*). We used a semi-automatic tracking method to find as long and as complete matched tracks as possible, for 6 of the most prominent tracks in the data, $j = 1, \ldots, 6$, i.e. $d_{i,j} = d_{i,k(i,j)}$. As can be seen in figures of Fig. 2, it is relatively straightforward to determine the travel times for the direct path from the single stationary transmitter to the moving receiver. As we will see later on the five other tracks correspond to reflections in roughly planar structures (walls) in the building. Each such path can thus be considered as originating from a stationary transmitter in an unknown (reflected) position. For 387 of these 404 time instants i a matched distance can be found to all 6 (real or virtual) transmitters. After computing $\bar{\mathbf{D}}$ as in Algorithm 4.1 from the 387×6 measurement matrix, it is observed that $\bar{\mathbf{D}}$ is almost of rank 2, which indicates that either (i) the receiver motion is roughly planar or (ii) the directions n_j to the transmitters are roughly planar.

Fig. 1. Overview of the measured scenario. Tx antenna in front and Rx antenna in the back.

The planar version of Algorithm 4.1 (planar version) is then used to obtain an initial estimate of $(\mathbf{r}_i, \mathbf{n}_j, o_j)$, which is used as a starting point for a non-linear least squares refinement of the parameters according to

$$(\mathbf{r}_i, \mathbf{n}_j, o_j) = \mathrm{argmin}_{\mathbf{r}_i, \mathbf{n}_j, o_j, |\mathbf{n}_j|=1} \sum_{i,j} |d_{i,j} - (\mathbf{r}_i^T \mathbf{n}_j + o_j)|^2. \tag{2}$$

The optimization is performed using the Levenberg-Marquart algorithm. Here we exploit analytic computations of both the residuals and the Jacobian. The least squares estimate is optimal if the measurement errors are independent Gaussian of equal variance. In practice it seems that the stronger peaks can be measured with lower variance. A future improvement would be to incorporate this in the process.

C. Position Estimates

The resulting estimated receiver motion is shown in Fig. 4 (*left*). Note that since the tracked paths all correspond to reflections in the horizontal plane (mainly walls), we found no reflections in the floor or ceiling, only the planar coordinates of the motion can be estimated. We believe that the reason that we find no reflections from the ceiling or floor is that the antenna patterns are fairly omnidirectional in the horizontal plane, but have a very low gain in the elevation angles close to 0 or 180 degrees. Due to this, the vertical motion cannot be obtained.

Once the initial estimate has been found for 387 of the 404 receiver positions, it is straightforward to extend the solution to all receiver positions and to additional transmitter positions. In our experiments we initialized these additional

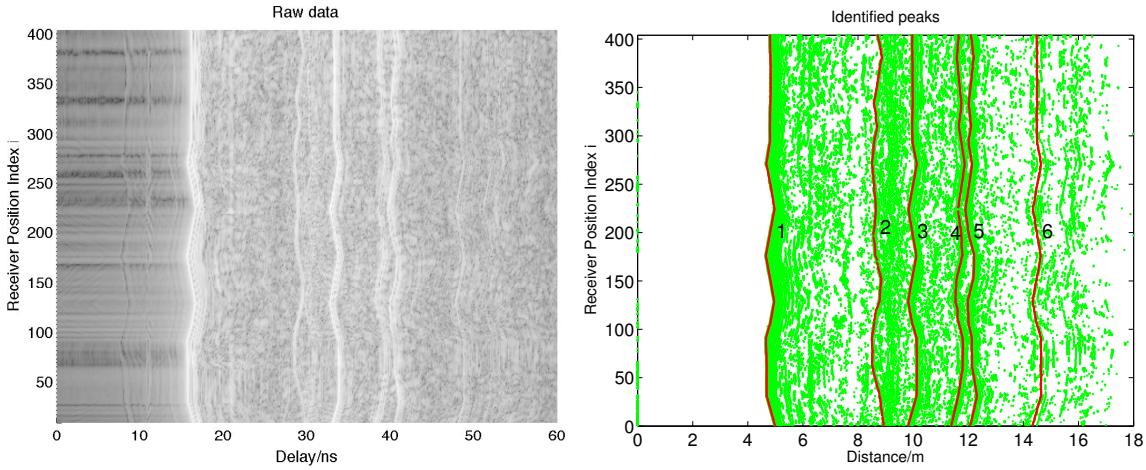

Fig. 2. Left: Matching strength between transmitted signal and received signal for each receiver position index i and each time delay. Notice that the strong peaks form tracks along the i-direction. Right: 100 strongest peaks (green) and the 6 best tracks (red) for each receiver position index i.

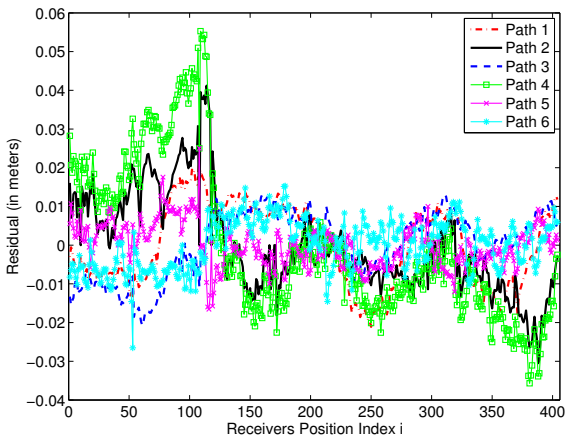

Fig. 3. Residuals between the estimated distances $\mathbf{r}_i^T \mathbf{n}_j + o_j$ and the measured distances $d_{i,j}$ after non-linear least squares optimization. Notice that the residuals are in the order of one centimeter.

17 receiver positions by linear techniques and refined the whole reconstruction using non-linear minimization. Notice that for the non-linear optimization it is possible to refine all parameters even if there are missing data simply by letting the sum in (2) be over all index pairs (i, j) for which there are measurements.

As a final step, we implemented a RANSAC approach, cf. [13], for finding additional multipath component matches. In this step we exploited the fact that such multipath component tracks are constrained to two parameters (θ, w), i.e.

$$d_i \approx \mathbf{r}_i^T \begin{pmatrix} \cos\theta \\ \sin\theta \end{pmatrix} + w. \tag{3}$$

Here the changing the parameter w corresponds to horizontal translations in Fig. 2 (*right*) and changing parameter θ corresponds to changing the shape of the matched curve. In the RANSAC loop, one iterates on (i) hypothesizing that two peaks correspond to the same transmitter, (ii) for such a hypothesis one then calculates the two parameters (θ, w) and thus the corresponding matched curve and finally (iii) assessing how many additional matches this curve contains within a threshold. By iterating (i)-(iii) and choosing the matched curve with the most inliers one can obtain additional multipath component matches. Again once a good inlier set has been found it is refined with non-linear optimization (2).

The final reconstruction is shown in Fig. 4 (*right*). In the figure is shown both the real transmitter location $\mathbf{s}_1$ as a square, the reflected transmitter locations $\mathbf{s}_2 \ldots \mathbf{s}_6$ as circles and the receiver positions $\mathbf{r}_i$ as dots. Note that the receiver motion is relatively small and difficult to perceive in this figure. In the figure we have also illustrated the geometry of the reflective surfaces, which in this case act as the major scatterers.

In order to make a comparison between ground truth motion $\mathbf{r}_{\text{true},i}$ and the estimated motion $\mathbf{r}_i$, we first rotate and translate the ground truth motion, i.e. we optimize

$$(\mathbf{R}, \mathbf{b}) = \operatorname{argmin}_{\mathbf{R},\mathbf{b},\mathbf{R}^\mathbf{T}\mathbf{R}=\mathbf{I}} \sum_{\mathbf{i}} |\mathbf{r_i} - (\mathbf{R}\mathbf{r}_{\text{true},\mathbf{i}} + \mathbf{b})|^{\mathbf{2}} \tag{4}$$

and then set

$$\mathbf{r}_{\text{fit},i} = \mathbf{R}\mathbf{r}_{\text{true},i} + \mathbf{b}. \tag{5}$$

In Fig. 4 (*left*) we show both the estimated receiver positions $\mathbf{r}_i$ and overlaid the fit $\mathbf{r}_{\text{fit},i}$ of the ground truth motion. The estimated standard deviation (RMS error) for $n = 404$ receiver positions

$$\sigma^\star = \sqrt{\frac{1}{(n-3)} \sum_{i=1}^{n} |\mathbf{r}_{\text{fit},i} - \mathbf{r}_i|^2} \tag{6}$$

was 1.34 cm. Notice that most residuals (cf. Fig. 3) are in the order of ± 1 cm, whereas the residuals corresponding to transmitter $j = 4$ and receivers $i \approx 50 \ldots 120$ there are significantly larger residuals. One hypothesis here is there are matching errors here that influence the reconstruction. The receiver positions $i \approx 50 \ldots 120$, correspond to the wiggly upper part in Fig. 4 (*left*).

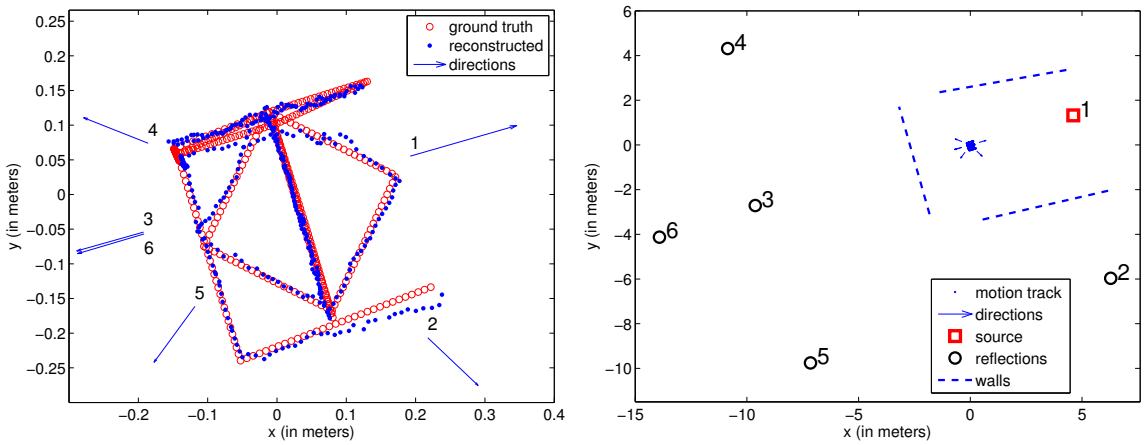

Fig. 4. Left: ground truth motion (red circles) and the estimated receiver positions r_i (blue dots, 387 of the 404 measurement positions). In the figure is also shown the directions to the real and virtual antenna positions ($-\mathbf{n}_j$'s). Right: Positions of the 'source' (red square) and virtual (reflected) transmitters (black circles). The hypothesized reflective wall positions based on the relative positions between source and reflections are also plotted.

In this initial investigation the movements were done in a small volume to ensure that the major MPCs show small variation over the movements. Future work include improved state space tracking also allowing death and birth processes of MPCs. We will also investigate the performance for the NLOS case.

VI. Conclusions

In this paper we have studied how anchor-free indoor localization with roughly centimeter precision can be obtained using UWB measurements from a single transmitter in an unknown environment to a moving antenna. The absolute travel times of the MPCs from the transmitter to the receivers are measured using a VNA both for the direct path and for reflections in natural indoor features, such as walls. The reconstruction of both receiver positions and real and virtual (reflected) transmitters is cast as a structure from motion problem. Such problems have received increased attention lately and the knowledge on how to solve such problems are refined. Using a combination of factorization, calibration and non-linear least squares optimization we obtain such estimates of receiver and transmitter positions. A crucial problem here is also the correspondence problem, i.e. the matching of identified distances to transmitter ids. In the paper we have used a semi-automatic approach to get an initial estimate. We have also shown how such structure from motion algorithms can be used in a RANSAC fashion to obtain additional matched tracks. Future research includes the development of algorithms for automatic matching already for the initial estimate.

Acknowledgments

The authors would like to thank Farzaneh Firouzabadi for her contributions regarding the measurements and delay extractions. The research leading to these results has received funding from the strategic research projects ELLIIT and eSSENCE, and Swedish Foundation for Strategic Research projects ENGROSS, VINST(grant no. RIT08-0043) and Center for High Speed Wireless Communication.

References

[1] S. Gezici, Z. Tian, G. Giannakis, H. Kobayashi, A. Molisch, H. Poor, and Z. Sahinoglu, "Localization via ultra-wideband radios: a look at positioning aspects for future sensor networks," *IEEE Signal Processing Magazine*, vol. 22, no. 4, pp. 70 – 84, July 2005.

[2] D. Dardari, A. Conti, U. Ferner, A. Giorgetti, and M. Z. Win, "Ranging with ultrawide bandwidth signals in multipath environments," *Proceedings of the IEEE*, vol. 97, no. 2, pp. 404–426, 2009.

[3] Y. Shen and M. Z. Win, "Fundamental limits of wideband localization-part i: a general framework," *Information Theory, IEEE Transactions on*, vol. 56, no. 10, pp. 4956–4980, 2010.

[4] P. Meissner, D. Arnitz, T. Gigl, and K. Witrisal, "Analysis of an indoor UWB channel for multipath-aided localization," in *IEEE International Conference on Ultra-Wideband, 2011*, Sept. 2011, pp. 565 –569.

[5] P. Meissner, C. Steiner, and K. Witrisal, "UWB positioning with virtual anchors and floor plan information," in *7th Workshop on Positioning Navigation and Communication (WPNC),*, March 2010, pp. 150 –156.

[6] H. Stewénius, "Gröbner basis methods for minimal problems in computer vision," Ph.D. dissertation, Lund University, Sweden, 2005.

[7] M. Pollefeys and D. Nister, "Direct computation of sound and microphone locations from time-difference-of-arrival data," in *ICASSP*, 2008.

[8] M. Crocco, A. Del Bue, and V. Murino, "A bilinear approach to the position self-calibration of multiple sensors," *Trans. Sig. Proc.*, vol. 60, no. 2, pp. 660–673, Feb. 2012. [Online]. Available: http://dx.doi.org/10.1109/TSP.2011.2175387

[9] S. Thrun, "Affine structure from sound," in *Proceedings of Conference on Neural Information Processing Systems (NIPS)*. Cambridge, MA: MIT Press, 2005.

[10] Y. Kuang, E. Ask, S. Burgess, and K. Åström, "Understanding TOA and TDOA network calibration using far field approximation as initial estimate," in *ICPRAM*, 2012.

[11] S. Burgess, Y. Kuang, and K. Åström, "Node localization in unsynchronized time of arrival sensor networks," in *International Conference on Pattern Recognition, Tsukuba Science City, Japan*, 2012.

[12] T. Santos, J. Karedal, P. Almers, F. Tufvesson, and A. Molisch, "Modeling the ultra-wideband outdoor channel: Measurements and parameter extraction method," *IEEE Transactions on Wireless Communications*, vol. 9, no. 1, pp. 282 –290, January 2010.

[13] M. A. Fischler and R. C. Bolles, "Random sample consensus: a paradigm for model fitting with applications to image analysis and automated cartography," *Communications of the ACM*, vol. 24, no. 6, pp. 381–95, 1981.

[14] N. Michelusi, U. Mitra, A. F. Molisch, and M. Zorzi, "UWB sparse/diffuse channels, part i: Channel models and bayesian estimators," *IEEE Transactions on Signal Processing*, vol. 60, no. 10, pp. 5307 – 5319, Oct. 2012.

[15] R.-M. Cramer, R. Scholtz, and M. Win, "Evaluation of an ultra-wide-band propagation channel," *IEEE Transactions on Antennas and Propagation*, vol. 50, no. 5, pp. 561 – 570, May 2002.